OPTICAL PROPERTIES OF SnS AND SnSe

A MASTER'S THESIS

in

Engineering of Physics

University of Gaziantep

by

Beşire GÖNÜL (ARPA)

February, 1991

Approval of the Graduate School of Natural and Applied Science

Prof.Dr. Mazhar ÜNSAL

I certify that this thesis statisfies all the requirements as a thesis for the degree of Master of Science in Engineering of Physics Department.

Assoc. Prof. Dr.Ata SELÇUK

Chairman of The Department

We certify that we have read this thesis and in our opinion it is fully adequate, in scope and quality, as a thesis for the degree of Master of Science in Engineering of Physics Department.

Assoc. Prof. Dr. İ.Engin Türe

Supervisor

Examining Committee in Charge

Assoc. Prof. Dr. Ata Selçuk

Assoc. Prof. Dr. İ. Engin Türe

Assist. Prof. Dr. Muktim Erdoğmuş

ABSTRACT

OPTICAL PROPERTIES OF SnS and SnSe

GÖNÜL (ARPA) Beşire
M.S. in Engineering of Physics
Supervisor: Assoc. Prof. Dr. İ.Engin TÜRE
February 1991, 46 pages

The optical transmission in the layered semiconductors of SnS and SnSe has been studied in the wavelength range of 200-1100 nm for the polarised light of $\epsilon \| \vec{a}$ and $\epsilon \| \vec{b}$, where $\vec{a}$ and $\vec{b}$ are the crystallographic axes within the cleavage plane. Indirect bandgaps of 1.24 and 1.17 eV for SnS and 0.74 and 0.8 eV for SnSe have been found for the two directions of the polarisations $\epsilon \| \vec{a}$ and $\epsilon \| \vec{b}$ respectively.

In the layered compound of SnSe, two indirect transitions (E_{i1} and E_{i2}) were identified as E_{i1}=1.14 ± 0.01 eV and E_{i2} = 1.26±0.01 eV for $\epsilon \| \vec{a}$ polarisation and E_{i1} = 1.12 ± 0.01 eV and E_{i2} = 1.22 ± 0.01 eV for $\epsilon \| \vec{b}$ polarisation.

It was found that the phonon assisted transitions in SnS required the participation of two phonons with energies of 0.03 eV and 0.075 eV for $\epsilon \| \vec{a}$ polarisation and 0.05 eV and 0.15 for $\epsilon \| \vec{b}$ polarisation.

The $K_a < K_b$ relation was found to be valid in SnSe whereas $K_a > K_b$ relation in SnS for the whole range of energies of incident light. The compounds of SnS and SnSe were found to be strongly anisotropic from the optical measurements of these compounds.

Keywords: Layered semiconductors, cleavage plane, optical transmission, absorption coefficient.

ÖZET

SnS ve SnSe'NİN OPTİK ÖZELLİKLERİ

GÖNÜL (ARPA) Beşire
Yüksek Lisans Tezi, Fizik Mühendisliği Bölümü
Tez Yöneticisi: Doç.Dr.İ.Engin Türe
Şubat 1991, 46 sayfa

SnS ve SnSe tabakalı yarıiletkenlerde optik geçişler 200-1100 nm dalga boyu aralığında $\mathcal{E}\|\vec{a}$ ve $\mathcal{E}\|\vec{b}$ yönlerinde polarize ışık için incelenmiştir. Burada $\vec{a}$ ve $\vec{b}$ vektörleri kristalin yarılma düzlemi içinde yer alan kristalografik eksenlerdir. İndirekt band aralıkları SnS için 1.24, 1.17 eV ve SnSe için 0.74 ve 0.8 eV sırasıyla $\mathcal{E}\|\vec{a}$ ve $\mathcal{E}\|\vec{b}$ polarizasyonları için elde edilmiştir.

SnSe tabakalı yarıiletkeninde iki indirekt geçiş, E_{i1} ve E_{i2}, $E_{i1} = 1.14 \pm 0.01$ eV ve $E_{i2} = 1.26 \pm 0.01$ eV olarak $\mathcal{E}\|\vec{a}$ polarizasyonu için, $E_{i1} = 1.12 \pm 0.01$ ve $E_{i2} = 1.22 \pm 0.01$ eV $\mathcal{E}\|\vec{b}$ polarizasyonu için ortaya çıkarılmıştır.

SnS'de phonon yardımlı geçişlerin $\mathcal{E}\|\vec{a}$ polarizasyonunda 0.03 eV ve 0.075 eV, $\mathcal{E}\|\vec{b}$ polarizasyonunda 0.05 eV ve 0.15 eV enerjilerine sahip iki phonon katkısına gerek duyduğu bulunmuştur.

$K_a < K_b$ bağıntısının gelen ışığın bütün dalga boyları için SnSe'de geçerli olmasına karşılık SnS'de $K_a > K_b$ bağıntısının geçerli olduğu bulunmuştur. Optik ölçmelerden SnS ve SnSe bileşiklerinin hayli anizotropik olduğu anlaşılmıştır.

Anahtar kelimeler: Tabakalı yarıiletkenler, kayma düzlemi, optik geçirgenlik, absorplanma katsayısı.

ACKNOWLEDGEMENT

I would like to express my gratitude to my supervisor Assc. Prof. Dr. I. Engin Ture, for his valuable guidance and encouragement throughout the course of the research. I am particularly indebted to Prof. Dr. Mustafa Merdan for the initiation of this study before his departure from the department to his new duty at Selcuk University.

I also would like to thank my parents and my husband for their constant support and encouragement during this study.

TABLE OF CONTENTS

	Page
ABSTRACT	iii
ÖZET	iv
ACKNOWLEDGEMENT	v
LIST OF TABLES	vii
LIST OF FIGURES	viii
1.INTRODUCTION	1
1.1. Introduction	1
1.2. Optical Properties of SnS and SnSe	5
2.MATERIALS AND METHODS	7
2.1. Preperation of Samples	7
2.2. Experimental Technique	7
2.3. The Measurement System	10
2.4. Specifications of The Spectrometer	10
2.5. Intensity of The Transmitted Light	12
2.6. Calculation of Absorption Coefficient	13
2.7. Determination of The Energies of Indirect Gaps	14
3.INTERBAND TRANSITIONS	15
3.1. Introduction	15
3.2. The Region Near The Absorption Edge	15
3.3. Properties of SnS	18
3.4. Properties of SnSe	20
4.EXPERIMENTAL RESULTS AND CALCULATIONS	27
4.1. Introduction	27
4.2. Tin Selenide	27
4.3. Tin Sulphide	33
5.DISCUSSION AND CONCLUSION	40
5.1. Discussion	40
5.2. Conclusion	43
REFERENCES	45

LIST OF TABLES

Table		Page
1.	Lattice parameters of SnS and SnSe in ^{o}A	2
2.	Density, the linear temperature coefficient, the Hall mobility, and effective mass of holes for SnS and SnSe	4
3.	The mutual relations between the notations of the irreducible representations of the space group D_{2h}^{16} at the point Γ and the lines V and Λ by V-G and slater.	22
4.	Possible indirect interband transitions in SnSe deduced from the band structure	22
5.	Possible indirect interband transitions in SnSe deduced from the electronic energy band structure of SnSe	25
6.	The direct optical dipole selection rules for the D_{2h}^{16} group	26
7.	Steepness coefficients and energy values of the points of discontinuity for the absorption edge of SnS for two directions of light polarisations at 300 K	39
8.	Indirect bandgap energy and energy of phonons for SnS	39

LIST OF FIGURES

Figure		Page
1.	The primitive cell of a GeS-like compound	3
2.	Main unit and nameplate	8
3.	Optical system of the instrument	9
4.	Block diagram of the system	11
5.	Band structure of SnSe	21
6.	Two types of most probable virtual processes corresponding to each indirect transition listed in Table 4	23
7.	a K versus λ of SnSe for $\varepsilon \parallel \vec{a}$ and $\varepsilon \parallel \vec{b}$ polarisations	28
	b K versus E of SnSe for $\varepsilon \parallel \vec{a}$ and $\varepsilon \parallel \vec{b}$ polarisations	29
8.	$(KE)^{1/2}$ versus E of SnSe for $\varepsilon \parallel \vec{a}$ and $\varepsilon \parallel \vec{b}$ polarisations.	31
9.	$(KE)^{1/3}$ versus E of SnSe for $\varepsilon \parallel \vec{a}$ and $\varepsilon \parallel \vec{b}$ polarisations	32
10.	$(KE)^{1/2}$ versus E of SnSe in polarised light at room temperature	34
11.	K versus E of SnSe in polarised light for a) $\parallel \vec{a}$ and b) $\parallel \vec{b}$	34
12.	K versus λ of SnS for $\varepsilon \parallel \vec{a}$ and $\varepsilon \parallel \vec{b}$ polarisations	35
13.	$(Kh\nu)^{1/2}$ versus $h\nu$ of SnS for $\varepsilon \parallel \vec{a}$ and $\varepsilon \parallel \vec{b}$ polarisations	36
14.	$\alpha(Kh\nu)^{1/2} / \alpha(h\nu)$ versus $h\nu$ of SnS for $\varepsilon \parallel \vec{a}$ and $\varepsilon \parallel \vec{b}$ polarisatons	38

CHAPTER ONE

INTRODUCTION

1.1 Introduction

Layer compounds are characterised by their anisotropic properties along different crystallographic directions. Layer compounds crystallise as thin plates which is a characteristic feature of these materials. Thin plate form is appropriate for the investigation of the optical and electrical properties of layer compounds. This form is also suitable for the determination of the crystal structure defects. Each crystal is composed of thin layers stacked upon each other. Within each layer, the atoms are bound predominantly covalent forces. The bond between the layers are extremely weak due to the Van der Waal's force and this provides a perfect cleaving along the cleavage plane in order to obtain very thin plates. This property is found to be very valuable by providing a favourable surface to the bulk ratio for the measurement of the optical characteristics of the layers.

Tin Sulphide (SnS) and Tin Selenide (SnSe) are isomorphous and they are considered to be layer-like materials. They both crystallise as a deformed Sodium Chloride structure. The original structure assignment was first made by Hoffmann [1], who described the unit cell as orthorhombic D_{2h}^{16} composed of four molecules, with lattice parameters a=3.98 °A,

b=4.33 °A, c=11.18 °A. In this structure the Sn atom is surrounded by six S atoms, three at a short distance (2.68 °A) with the interatomic directions almost perpendicular to each other (88° 10' ; 88° 10' and 95° 8') and three atoms at a somewhat larger distance (3.38 °A) with the interatomic directions at angles 118°, 118°, and 75° respectively, and forming an angle of 78° with the interatomic directions of the first group of S atoms. Thus we can describe this structure along the $\vec{c}$-axis, as composed of double layers.

From the crystallographic point of view, SnS and SnSe are characterized by three axes $\vec{a}$, $\vec{b}$, $\vec{c}$ perpendicular to each other [2]. The axes $\vec{a}$ and $\vec{b}$ (a>b) lay in the cleavage plane, the third one, $\vec{c}$, is perpendicular to this plane. It holds $a \approx b$ and c is much greater than a and b (Table I).

Table I. Lattice parameters of SnS and SnSe in A.

	SnS	SnSe
a	3.98	4.46
b	4.33	4.19
c	11.18	11.57
Source	[4]	[3]

It should be noted that this choice of the axes denotation is not the only one used in literature (see e.g.[3], where b>a>c, so that $\vec{a}$ and $\vec{c}$ lay in the cleavage plane while $\vec{b}$ is perpendicular to it). Nevertheless, the former definition predominates in the more recent literature and it has been used throughout this study. GeS and GeSe are also belong to the layer-like materials and the primitive cell of a GeS-like compound is given in Fig.1 [2].

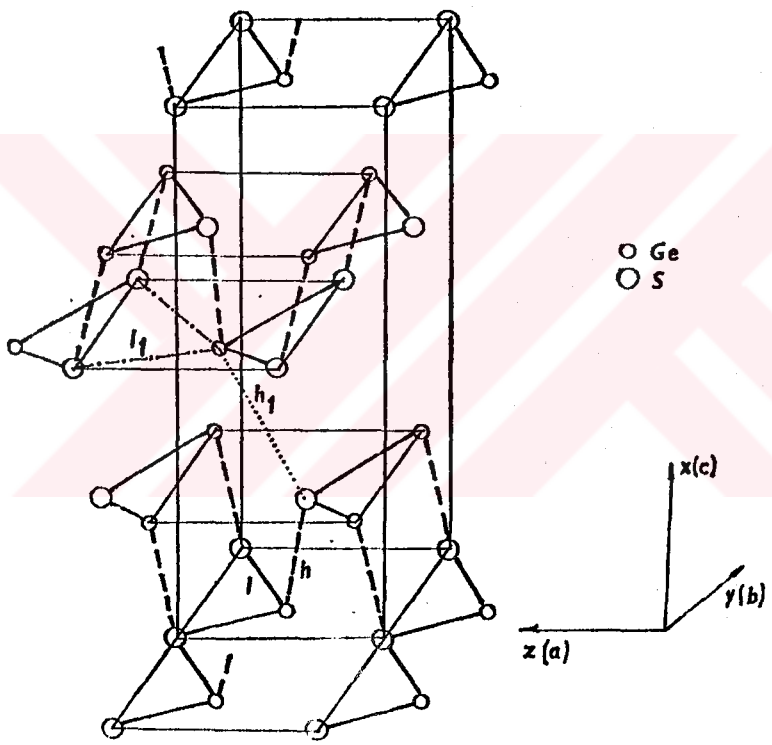

Fig.1. The primitive cell of a GeS-like compound. Each Ge atom is surrounded by 6 Sulphur atoms (and vice versa) in a distorted octahedral arrangement. The lengths of 6 Ge-S bonds are: one at h =2.47 A (---), two at l=2.64 A (_ _), one at h_1=2.91 A (...), and two at l_1=3.00 A (-.- -.).

As these materials can easily be cleaved along the $(\vec{a},\vec{b})$ plane and it is rather easy to prepare very thin layers of about 55 μm from the crystal, it is possible to study optical properties in polarised light for $\mathcal{E} \| \vec{a}$ and $\mathcal{E} \| \vec{b}$ orientations without any problem. On the other hand, it is very difficult to prepare the samples in other orientations such as $(\vec{a},\vec{c})$ and $(\vec{b},\vec{c})$. For this, the crystal should be cut along $(\vec{a},\vec{c})$ or $(\vec{b},\vec{c})$ plane and then to be polished and etched in order to prepare the samples. Another difficulty of preparing samples in other directions rather than $(\vec{a},\vec{b})$ plane is due to the softness of the material. As a consequence, the surface quality of the samples which are prepared in $(\vec{a},\vec{c})$ and $(\vec{b},\vec{c})$ planes are poorer than that of the surface prepared in $(\vec{a},\vec{b})$ plane. It is clear that the quality of surfaces become even more important when the optical measurements are concerned.

As it can be seen from the literature [2] , the grown crystals are always p-type having considerably high hole concentrations (mostly in the order of 10^{17} - 10^{18} cm^{-3}) and consequently with low resistivity.

The density, the linear temperature coefficient, the Hall mobility, and the effective mass of holes are summarised in table II [5].

Table II. Density (s), the linear temperature coefficient (α), the Hall mobility (μ_H), and effective mass of holes (m_j) for SnS and SnSe.

	S [g cm^{-3}]	α[$10^6 K^{-1}$]	μ_H[$cm^2 V^{-1} s^{-1}$]	m_j
SnS	5.08		μ_c=90	m_a 0.20
				m_b 0.20
				m_c 1.0
SnSe	6.179	α_a= -26	μ_c=-26	m* 0.15
		α_b= 35		
		α_c= 26		

PbS, PbSe, PbTe, and SnTe which belong to the rocksalt structure have been extensively studied, whereas, the layer compounds with distorted rocksalt structure of the orthorhombic space group (D_{2h}^{16}), namely GeS, GeSe, SnS, and SnSe have only recently received some attention. They are part of the small number of IV-VI compound semiconductors. Owing to their layer structure, they manifest strongly anisotropic vibrational properties.

1.2 Optical Properties of SnS and SnSe

The absorption spectra of SnS have been reported by Lambros et al. [4] near the absorption edge (0.55-1.55 eV) at 100 and 300 K. Reflectivity for both of the orientations within the cleavage plane has been measured by Eymard and Otto [6] in the range from 1.5 to 6.0 eV. Sobolev and Donetskich [7] have reported the reflectivity spectra from 1.5 to 12 eV at 77 and 300 K. Bletskan et al. [8] have studied the electroreflectance (ER) spectra in unpolarised light from 1.1 to 4.3 eV. Tyagai et al. [9] have described the results of the study of ER spectra in polarised light for $\mathcal{E} \| \vec{a}$ and $\mathcal{E} \| \vec{b}$ polarisations performed at RT in the range of 1.1 to 2.5 eV. Lukes et al. [2] have also studied the thermoreflectance (TR) and eletroreflectance (ER) spectra from 1 ? to 4.8 eV for polarisations $\mathcal{E} \| \vec{a}$ and $\mathcal{E} \| \vec{b}$.

The absorption coefficient of SnSe near the absorption edge has already been studied by several authors [10,11,12]. The TR and ER spectra of SnSe have been reported by Valiukanis et al.[13]. Lukes et al.

[14] have studied the absorption edge of SnSe in the energy range of 0.8-1.4 eV at 95 K and 295 K for either orientations in the cleavage plane. They have also studied the reflectivity spectra in the energy range of 0.5-5.5 eV, the absorption spectra in the near infrared (0.5-0.9 eV) at temperatures ranging from 95 to 295 K. The TR spectra at 95 and 320 K and ER spectra at 295 K have also been reported by the same authors.

The work on the optical properties of SnSe above 6 eV is very limited. There are only few reports concerning with the optical properties of SnSe below the absorption edge (far infrared region) and almost all of them are devoted to the measurements of the reflectivity spectra. It is evident that, the optical studies on these two materials are confined mostly in the near infrared region.

In this study the work on SnS and SnSe has been extended from 1.12 eV to 6.20 eV. As it can be seen from the studies summarised above, the transmission measurements have been carried out in a limited range of energies. In literature, the authors have reported the absorption spectra by using either thermoreflectance or electroreflectance measurements. In this work, the absorption coefficients and other related optical parameters of SnS and SnSe have been calculated by making use of transmission measurements in the range of 1.12-6.20 eV.

CHAPTER TWO
MATERIALS AND METHODS

2.1 Preparation of Samples

Thin layers ($d < 100\ \mu m$) of SnS and SnSe samples were prepared from single crystals by removing the surface layers with adhesive tapes in order to obtain very thin and as perfect as possible surfaces. Since the quality of single crystals of SnSe and especially SnS were not very good, the process of obtaining surfaces suitable for optical measurements was not easy.

2.2 Experimental Technique

A Jasco model 7800 spectrometer of LCD type was used for the measurements in ultraviolet, visible , and infrared regions (see Fig.2). The optical system of this instrument is shown in Fig.3. A Deuterium lamp was used in the ultraviolet and a Tungsten-Iodine lamp was used in the visible-to-near infrared regions of the spectrometric measurements as the light sources. A high order cut-off filter was put in the way of the light beam obtained one of the sources mentioned above. A monochromatic light was then obtained by using a concave diffraction grating in the monochromator. A beam splitter was also used in the way of the monochromatic light in order to be able to illuminate both the SnS or SnSe specimen and the reference sample or the silicon photodetector.

The samples were placed in special holders with the help of adhesive tapes and the intensities of the

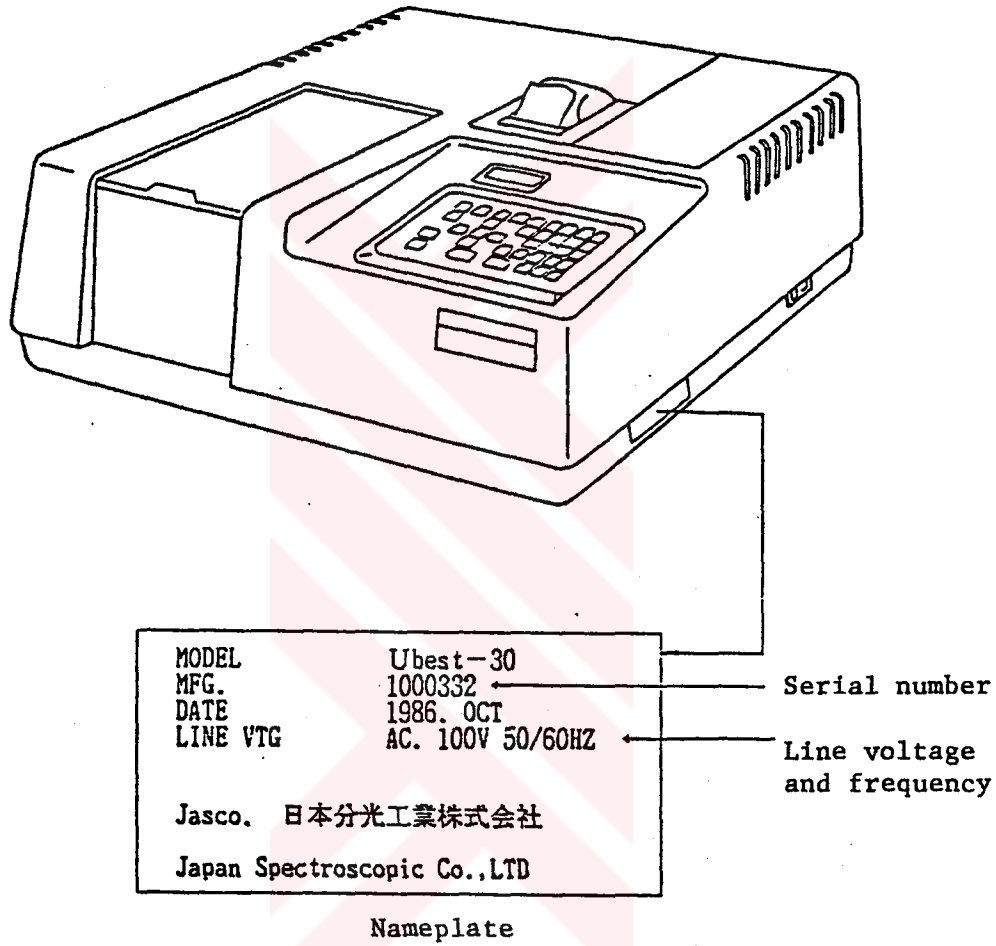

Fig.2. Main Unit and Nameplate

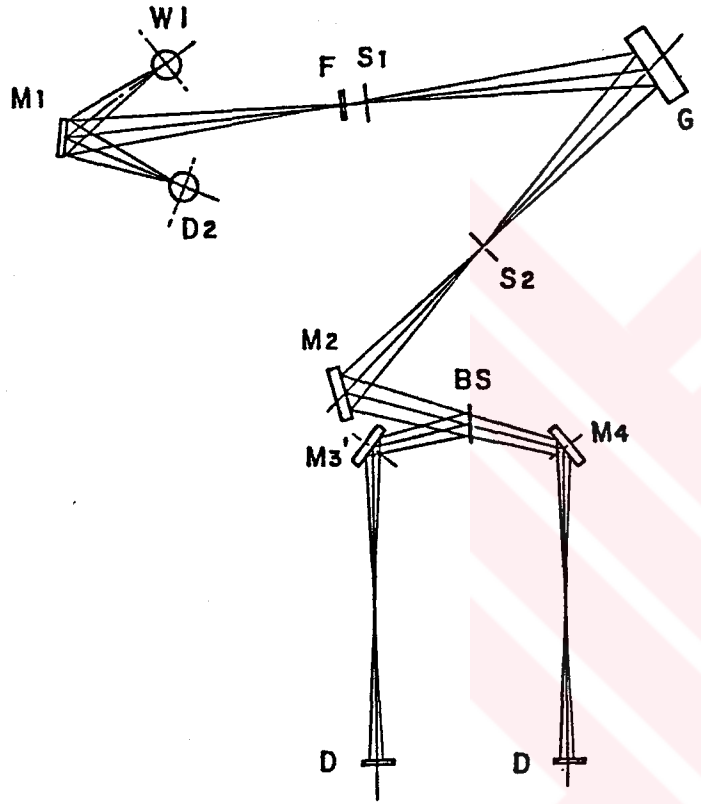

w_1: Tungsten iodine lamp

D_2: Deuterium lamp

M_1 to M_4: Mirror

F : Filter

S_1, S_2 : Slit

G : Concave difraction grating

BS: Beam splitter

D : Detector

Figure 3. Optical system of the instrument

transmitted light were measured by silicon photodetectors at room temperature. All the measurements have been carried out by using polarised light. The polariser was immediately put after the exit slit of the monochromator.

2.3 The Measurement System

The measurement system which was used in this study is shown in Fig.4. Following the conversion of light signal into an electrical signal by a photodetector and amplified the signal was subjected to A-D conversion. A microcomputer was then employed in order to process this data and provide an output.

2.4 Specifications of the Spectrometer (Jasco Model 7800)

Optical System	: Concave diffraction grating Double-beam monochromator
Light Source	: Deuterium discharge tube (200 nm to 350 nm) Tungsten iodine lamp (330 nm to 1100 nm)
Light Source Changeover Wavelength	: Wavelength can be selected at 330 or 350 nm
Wavelength Range	: 200 nm to 1100 nm
Wavelength Repeatability	: ± 0.1 nm
Wavelength Accuracy	: ± 0.5 nm
Spectrum Band Width	: 3 nm, fixed
Wavelength Display	: 1000.0 nm (0.1 nm)

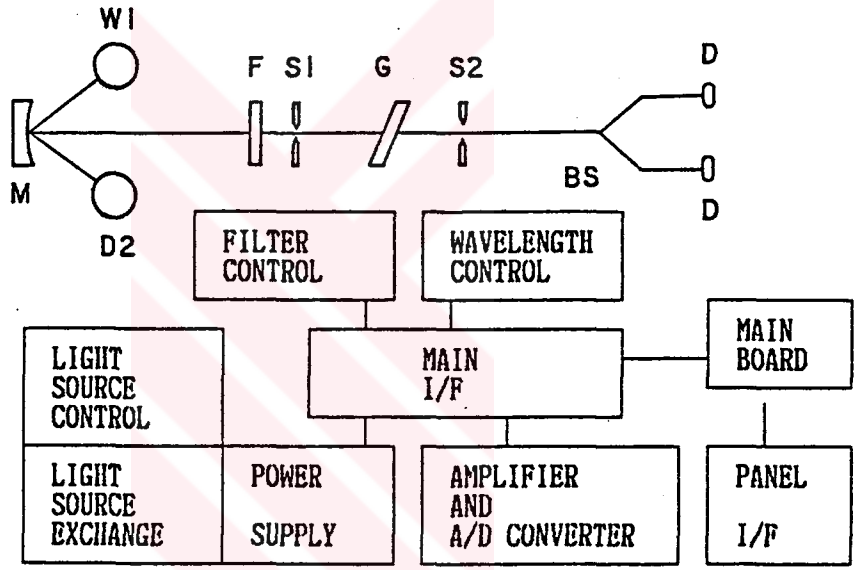

Fig.4. Block Diagram of The System

Measurement Range	: 0 to 2 Abs.
Measurement Display	: 0.0 to 200.0 %T 0.000 to 2.000 Abs. Can be displayed up to 000.00 %T 0.0000 Abs. by changeover
Measurement Reproducibility	: ± 0.001 Abs.(0 to 0.5 Abs.) ± 0.002 Abs. (0.5 to 1 Abs) ± 0.15 % T
Measurement Accuracy	: 0.005 Abs (0 to 1 Abs) ± 0.3 % T
Scan Speed	: 240,480,1200,2400 nm /Min
Stray Light	: 0.1 % (220,340 nm)
Base Line Flatness	: ± 0.001 Abs(200 to 1100 nm)
Base Line Stability	: ± 0.001 Abs/day
Clock Function	: Provided
Detector	: 2 Silicon photocells
Line Voltage	: 100,115,200,220,230,240 V
Dimensions and Weight	: 478 mm wide x 460 mm deep x 195 mm high , 15 kg.

2.5 Intensity of Transmitted Light

Transmittance of the samples has been determined by using sample-in sample-out method, point by point, at room temperature. In order to take more precise measurements the zero adjustment of the spectrometer has to be calibrated for each wavelength. The trans-

mission values obtained from the freshly cleaved surfaces were found to be different from the transmission values for the surfaces exposed to the air.

The intensity of a transmitted light is given by equation 2.1

$$I = I_o \exp(-Kx) \tag{2.1}$$

where, I is the intensity of the beam emerging, I_o is the intensity of the incident light ($I<I_o$), K is the absorption coefficient and x is the thickness of the sample. Equation 2.1 is a measure of the rate of loss of light from the incident beam.

2.6 Calculation of Absorption Coefficient (K)

Equation 2.1 can be used for the analysis of the transmission data and to calculate the absorption coefficient (K). When two samples having different thicknesses were used, the absorption coefficient can be calculated more precisely. The intensities for each sample can be written as

$$I_1 = I_o \exp(-Kx_1) \tag{2.2}$$

$$I_2 = I_o \exp(-Kx_2) \tag{2.3}$$

dividing equation (2.2) by equation (2.3) and taking logarithm of both sides, the following equation can be obtained

$$\ln\left(\frac{I_1}{I_2}\right) = K\,\Delta x \tag{2.4}$$

where $x=x_2-x_1$, so absorption coefficient K, becomes

$$K = \frac{\ln\left(\frac{I_1}{I_2}\right)}{\Delta x} \qquad (2.5)$$

2.7 Determination of the Energies of Indirect Gaps

The following procedure can be used for the determination of the indirect bandgaps;

a) decomposition of the curves KE=f(E) in the plane $(KE)^n$ versus E for n=1/2 or 1/3

b) numerical derivation of the curves KE=f(E) and identification of the gaps where the derivatives change abruptly.

The energy of the first indirect transition has been formed by means of first procedure. For higher transitions the second procedure (b) can be used. A pronounced break which gives the characteristic energy values on the K versus E curve can also be used for the determination of indirect energy gaps at higher transitions.

CHAPTER THREE

INTERBAND TRANSITIONS

3.1 Introduction

Although there are some features common to both the SnS and SnSe, the detailed study of the reports on the optical properties of these materials, in the region of interband transitions, leads to the conclusion that the absorptions of the materials are different near the absorption edge. It is well known that, some materials (i.e. GaAs, InSb) have direct transitions and others (AlAs, GaP) have indirect transitions between the valence and conduction bands. When this fact is taken into account, it is not unusual to find differences in the optical properties between SnS and SnSe.

3.2 The Region Near The Absorption Edge

The absorption coefficient (K) of a material is a function of the energy of the incident light. For a given photon energy (E) greater than the direct bandgap (E_{do}) of a material, the product of the absorption coefficient with the specific photon energy can be expressed by

$$KE = A(E - E_{do})^{1/2} \qquad (3.1)$$

in 3-D structure. Where A is a constant which is temperature,phonon energy and photon energy dependent. Similarly for direct forbidden transitions

$$KE = A' (E - E_{do})^{3/2} \qquad (3.2)$$

can be written. When indirect transitions are considered, the above equation can be written as follows

$$KE = A_j(E - E_{ij} \pm E_{pj})^2 \qquad (3.3)$$

for allowed transitions, and

$$KE = A'_j (E - E_{ij} \pm E_{pj})^3 \qquad (3.4)$$

for forbidden transitions. Where, E_{ij} is the j-th indirect energy-gap, E_{pj} is the energy of phonons assisting in indirect transitions. It should be noted that, the above equations are valid at a constant temperature. It should also be noted that, the above equations give a reasonable accuracy in the calculation of absorption coefficients, when the energy bands of a material are parabolic.

The absorption coefficient near the absorption edge may be expressed as [2]

$$K_t(E) = K_b(E) + K_c(E) \qquad (3.5)$$

where, $K_t(E)$ is the total absorption coefficient determined experimentally. $K_c(E)$ is the absorption due to interband transitions and $K_b(E)$ represents the background absorption which may be due to impurities, native defects in bulk or at the surface of the material and K_b strongly depends on the energy of the incident light [15]. The absorption due to the inter-

band transitions , K_c (E), can be calculated as

$$K_c(E) = K_t(E) - K_b(E) \qquad (3.6)$$

where K_b(E) may be found from the extrapolation of the absorption coefficient below the absorption edge, when (KE) is drawn against the photon energy. The value of K_c(E) can then be calculated by using equations (3.1)-(3.4). Eq.(3.3) and (3.4) can be rewritten as

$$K_c(E) = \sum_{l=1}^{L} \{ B_{na} \frac{1}{e^{\frac{E_{pl}}{kT}} - 1} (E - E_{ij} + E_{pl})^n + B_{ne} \frac{1}{1 - e^{-\frac{E_{pl}}{kT}}} (E - E_{ij} - E_{pl})^n \} \qquad (3.7)$$

for K_c(E) when the indirect transitions are considered. B_{na} and B_{ne} are temperature dependent coefficients representing the processes with phonon absorption and phonon emission, E_{pl} is the energy of phonon assisting in the transition. There may be more phonons (L) assisting in the same transition; n=2 or 3 for indirect allowed and indirect forbidden transitions.

The procedure based on the expression of experimentally found K_c(E) values in the form $(K_c(E))^m = f(E)$ where m=1/2 or 1/3 for indirect allowed and indirect forbidden transition is applied to the most of the calculations. In the case of indirect transitions which is assisted with one phonon in the range of $(E-E_{pl})$ to

$(E+E_{pl})$, K_c^m can be written as

$$K_c^m = B_{ne} \frac{1}{1 - e^{\frac{E_{pl}}{kT}}} (E - E_{ij} - E_{pl}) = (K_{ie})^m \qquad (3.8)$$

3.3 Properties of SnS

Tin Sulphide is classified as an indirect semiconductor [16]. The bandgap of it lies in the vicinity of 1.2 eV. For indirect interband transitions the absorption coefficient is expressed as a sum of the terms in the form

$$K(T) = \frac{K_o(T)}{h\nu} [N_p (h\nu - E_g' + hw_i)^2 + (1+N_p)(h\nu - E_g' - hw_i)^2] \qquad (3.9)$$

where $h\nu$ is the photon energy, E_g' is the indirect bandgap energy, $K_o(T)$ is a parameter which varies slowly with temperature, while hw_i is the energy of a phonon of momentum such as to promote the electron from the maximum of the valence band to the minimum of the conduction band, and N_p is the number of the phonons involved. From Bose-Einstein statistics which involves the energy of phonon, N_p has an expression in the form

$$N_p = \{\exp \frac{hw_i}{kT} - 1\}^{-1} \qquad (3.10)$$

Therefore, the first term in eq.3.9 describes processes involving phonon absorption, while the second term describes phonon emission. Thus in plotting the square root of the quantity $(Kh\nu)$ versus $h\nu$, a straight line is expected to resolve for each independent process. If the transitions are to be classified as indirect phonon assisted, the process should involve a more complex phonon participation than the one predicted by equation 3.9. This means that the different absorption processes are superimposed, and this is true regardless of the direction of the light polarization under investigation. Koshkin et al. [17] introduced the idea that complex absorption processes are revealed by investigating through graphical methods. This method has been employed using graphical differentiation of the absorption coefficient with respect to energy. A graph can be obtained by drawing $\partial(Kh\nu)^{1/2} / \partial(h\nu)$ versus $h\nu$. As it can be seen from this graph that the derivative $\partial (Kh\nu)^{1/2} / \partial(h\nu)$ is a step function of energy with several steps well defined in the range

$$E_o < h\nu < E_1$$
$$E_1 < h\nu < E_2$$
$$E_2 < h\nu < E_3$$
$$E_3 < h\nu < E_4$$
$$E_4 < h\nu \text{ and so on}$$

where the energy values of E_o, E_1, E_2, E_3 and E_4 indicate the points of discontinuity in the plot of $\partial(Kh\nu)^{1/2} / \partial(h\nu)$ versus $h\nu$. This analysis indicates that the dependence of absorption coefficient on energy and can be described by the equation of the form

$$(Kh\nu)^{1/2} = b_o + \sum_{i=1}^{n} b_i (h\nu - E'_g \pm E_i) \qquad (3.11)$$

where the coefficients b_i indicate the difference in height of the steps in the plot of $\partial (Kh\nu)^{1/2} / \partial (h\nu)$ versus $h\nu$. E'_g is the energy value of the indirect bandgap, while E_i is the energy value of the phonon involved in the process. If four steps are observed in both directions of polarization, there are two pairs of components associated with two different phonons participating in the absorption process. The energy gap value can be found from the threshold energies of these components. Thus the following relations can be used to calculate the energy of indirect gaps and the energy of phonons.

Indirect Energy Gaps

$$E'_{g1} = (E_o + E_3)\ /2$$
$$E'_{g2} = (E_1 + E_2)\ /2 \qquad (3.12)$$

Phonon Energies

$$hw_1 = (E_2 - E_1)\ /2$$
$$hw_2 = (E_3 - E_o)\ /2 \qquad (3.13)$$

3.4 Properties of SnSe

There exists two models of the band structure of SnSe, namely that by Ciucci et al. [18] and that by Gashimzade et al.[24]. The latter is reproduced in Fig.5. Both band structures are limited to some high symmetry lines only. It is along Λ in [18] (according to the Slater notation) and along V and Λ lines in [19] (according to the Valiukonis - Gashimzade (V - G) notation), which correspond to Λ and Δ lines according to the Slater notation. Both structures are

characterised by comparatively flat bands, both valence (v) and conduction (c) bands, with several local extrama energetically close to each other. It seems that even small changes of the atomic pseudopotentials may result in a mutual change of relative energies of these local extrama as is admitted in [13,19].

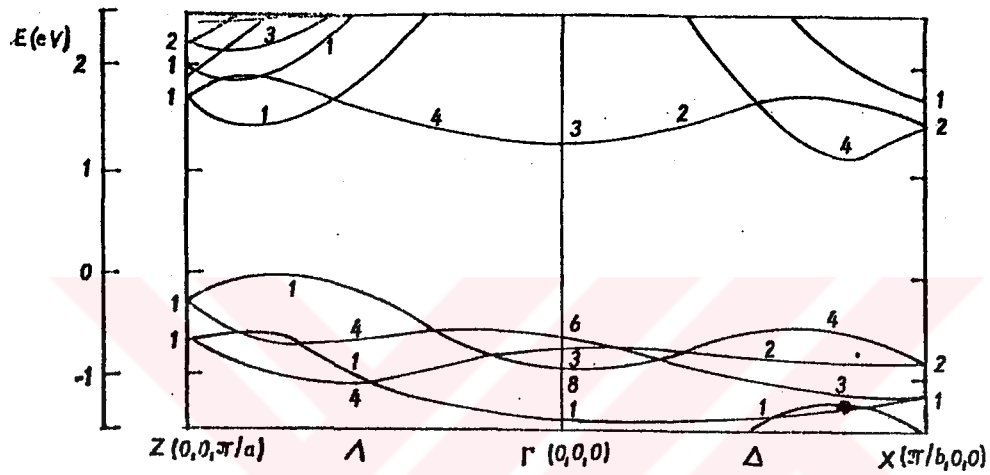

Fig. 5 Band structure of SnSe along the symmetry lines Λ and Δ [19].

The V - G notation is used in this study. The mutual relations between the notations of the irreducible representations of the space group D_{2h}^{16} at the point Γ and the lines V and Λ by Valiukonis and Gashimzade and by Slater are given in Table 3. The most promising candidates for the indirect transitions can be estimated from the band structure which was given in Fig.5. These are summarised in Table 4. Only two types of virtual processes given in Fig.6 contribute decisively to each considered indirect transition.

In order to interpret the experimental results,

Table 3. The mutual relations between the notations of the irreducible representations of the space group D_{2h}^{16} at the point Γ and the lines V and Λ by V-G and Slater.

notation by	symmetry point and/or line	irreducible representation
V-G	Γ	1 2 3 4 5 6 7 8
Slater	Γ	1 5 3 7 2 6 4 8
V-G	V	1 2 3 4
Slater	Λ	1 3 2 4
V-G	Λ	1 2 3 4
Slater	Δ	1 3 4 2

Table 4. Possible indirect interband transitions in SnSe deduced from the band structure given in [13] and [18] : a allowed, f forbidden.

Slater's notation	V-G's notation [5]	$\varepsilon \parallel a$	$\varepsilon \parallel b$
$\Lambda_1 \rightarrow \Delta_2$	$V_1 \rightarrow \Lambda_1$	a	a
$\Lambda_1 \rightarrow \Gamma_3$	$V_1 \rightarrow \Gamma_3$	a	f
$\Delta_2 \rightarrow \Gamma_3$	$\Lambda_1 \rightarrow \Gamma_3$	a	a
$\Delta_2 \rightarrow \Lambda_1$	$\Lambda_1 \rightarrow V_1$	a	a
$\Gamma_6 \rightarrow \Delta_2$	$\Gamma_6 \rightarrow \Lambda_1$	a	a
$\Gamma_6 \rightarrow \Lambda_1$	$\Gamma_6 \rightarrow V_1$	a	f

Fig.6 Two types of most probable virtual processes corresponding to each indirect transition listed in table 4: _____ radiative part, ------ phonon process.

it is need to know the selection rules for the indirect interband transitions in SnSe in Table 5. From the group - theoretical analysis of the lattice vibrations of SnSe alone it follows that in SnSe there are phonons of all symmetries inside the Brillouin Zone (BZ) [20]. Since the primitive cell of GeS - like semiconductors is formed by eight atoms there are twenty - four phonon branches of which three are acoustic and twenty - one optical ones. A factor - group analysis predicts that among the twenty - one optical phonons two are inactive, seven are infrared active, and twelve are Raman active. Special attention should be paid to polar modes characterised by the TO - LO splitting. When the polariton effects are not considered, the polar optical phonon branches in the orthorhombic crystal are non-analytic at the BZ centre, i.e. the energies of the zone-centre polar optical phonons depend on the direction the Γ point is approached along, and there appear more phonon energy levels at the Γ point than predicted by the factor-group analysis. Hence it is always possible to find an allowed phonon due to which the electron in the conduction band and/or the hole in the valence band is scattered between different points of the BZ, and the selection rules of the indirect transitions in SnSe are, therefore, determined by their radiative parts only. The selection rules for dipole vertical interband transitions for the D_{2h}^{16} group are listed in table 6. Using them and considering the two mentioned types of virtual processes shown in figure 6. It has been come to the conclusion in table 5.

Table 5. Possible indirect interband transitions in SnSe deduced from the electronic energy band structure of SnSe shown in fig.5.

a $\xrightarrow{i}$ radiative part allowed for i polarisation (i=a,b)

b $\xrightarrow{e}$ scattering of electron in the conduction band

c $\xrightarrow{h}$ scattering of hole in the valence band

a allowed , f forbidden.

Indirect transition	Two types of virtual processes		Selection rules[c]	
	Radiative (interband) part[a]	Electron and/or hole scattering due to phonon[b]	Polarization	
			$\mathcal{E} \parallel a$	$\mathcal{E} \parallel b$
$\Lambda_1^v \rightarrow \Delta_2^c$	$\Lambda_1^v \xrightarrow{a} \Lambda_1^c$ $\Delta_2^v \xrightarrow{b} \Delta_2^c$	$\Lambda_1^c \xrightarrow{e} \Delta_2^c$ $\Delta_2^v \xrightarrow{h} \Lambda_1^v$	a	a
$\Lambda_1^v \rightarrow \Gamma_3^c$	$\Lambda_1^v \xrightarrow{a} \Lambda_1^c$ $\Gamma_6^v \xrightarrow{a} \Gamma_3^c$	$\Lambda_1^c \xrightarrow{e} \Gamma_3^c$ $\Gamma_6^v \xrightarrow{h} \Lambda_1^v$	a	f
$\Delta_2^v \rightarrow \Gamma_3^c$	$\Delta_2^v \xrightarrow{b} \Delta_2^c$ $\Gamma_6^v \xrightarrow{a} \Gamma_3^c$	$\Delta_2^c \xrightarrow{e} \Gamma_3^c$ $\Gamma_6^v \xrightarrow{h} \Delta_2^v$	a	a
$\Delta_2^v \rightarrow \Lambda_1^c$	$\Delta_2^v \xrightarrow{b} \Delta_2^c$ $\Lambda_1^v \xrightarrow{a} \Lambda_1^c$	$\Delta_2^c \xrightarrow{e} \Lambda_1^c$ $\Lambda_1^v \xrightarrow{h} \Delta_2^c$	a	a
$\Gamma_6^v \rightarrow \Delta_2^c$	$\Gamma_6^v \xrightarrow{a} \Gamma_3^c$ $\Delta_2^v \xrightarrow{b} \Delta_2^c$	$\Gamma_3^c \xrightarrow{e} \Delta_2^c$ $\Delta_2^v \xrightarrow{h} \Gamma_6^v$	a	a
$\Gamma_6^v \rightarrow \Lambda_1$	$\Gamma_6^v \xrightarrow{a} \Gamma_3^c$ $\Lambda_1^v \xrightarrow{a} \Lambda_1^c$	$\Gamma_3^c \xrightarrow{e} \Lambda_1^c$ $\Lambda_1^v \xrightarrow{h} \Gamma_6^v$	a	f

Table 6. The direct optical dipole selection rules for the D_{2h}^{16} group.

Symmetry points and lines	$\mathcal{E} \parallel a$	$\mathcal{E} \parallel b$	$\mathcal{E} \parallel c$
Γ	1–8 2–7 3–6 4–5	1–4 2–3 5–8 6–7	1–6 2–5 3–8 4–7
U	1–8 2–7 3–6 4–5	1–4 2–3 5–8 6–7	1–7 2–8 3–5 4–6
Δ	1–2 3–4	1–1 2–2 3–3 4–4	1–4 2–3
F	1–3 2–4	1–1 2–2 3–3 4–4	1–4 2–3
Σ, A, C, E	1–2 3–4	1–4 2–3	1–1 2–2 3–3 4–4
A, G	1–1 2–2 3–3 4–4	1–2 3–4	1–4 2–3
T, S	1–2	1–2	1–1 2–2
Y, R	1–2	1–1 2–2	1–1 2–2
X, Z	1–1 2–2	1–2	1–1 2–2
D, B, H, Q	1–1	1–1	1–1

CHAPTER FOUR

EXPERIMENTAL RESULTS AND CALCULATIONS

4.1 Introduction

The direct and indirect interband transitions of SnS and SnSe were investigated at photon energy in the range of 1.12-6.20 eV in this work. The optical spectra for the two materials have been analyzed and the band-gap energies for each material were obtained from this study. A more detailed analysis of indirect transitions for SnSe was carried out compared to the indirect transitions for SnS.

4.2 Tin Selenide (SnSe)

Transmission measurements were performed by using several samples of SnSe having different thicknesses. The thickness of the samples range from 0.065 mm to 9000 μm, and these are cleaved from a p-type SnSe crystal. Measurements were carried out for orientations $\mathcal{E}\|\vec{a}$ and $\mathcal{E}\|\vec{b}$ in polarised light.

The curves $K=f(\lambda)$ and $K=f(E)$ are given in figure 7.a and 7.b respectively for both orientations $\mathcal{E}\|\vec{a}$ and $\mathcal{E}\|\vec{b}$ at room temperature, where K is the absorption coefficient, λ is the wavelength of the incident light and E is the energy of the incident light.

The dependence of $(KE)^{1/2}= f(E)$ (see fig.8) and $(KE)^{1/3}=f(E)$ (see fig.9) have been used to determine the

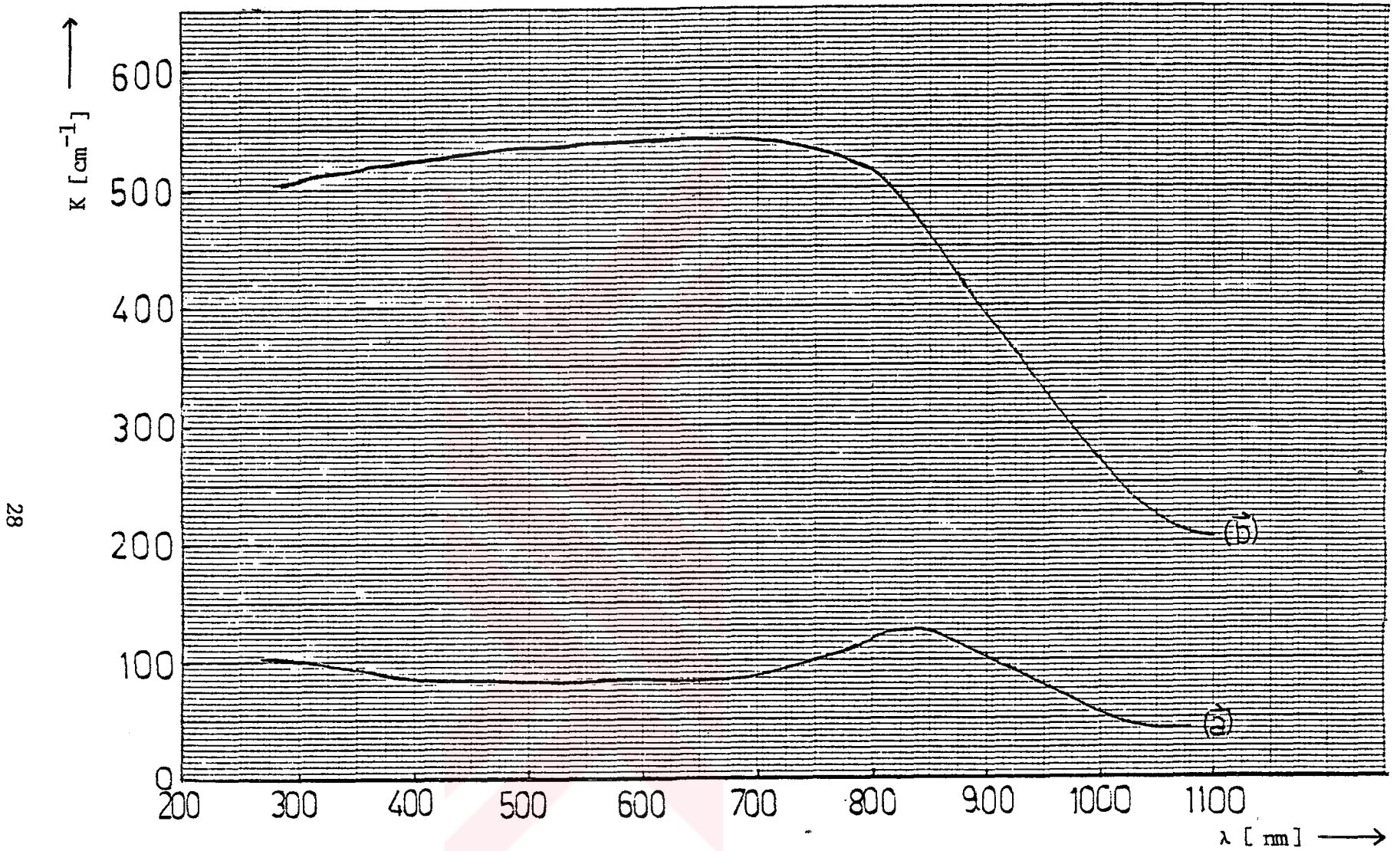

Fig.7a K versus λ of SnSe for $\mathcal{E} \| \vec{a}$ and $\mathcal{E} \| \vec{b}$ polarisations.

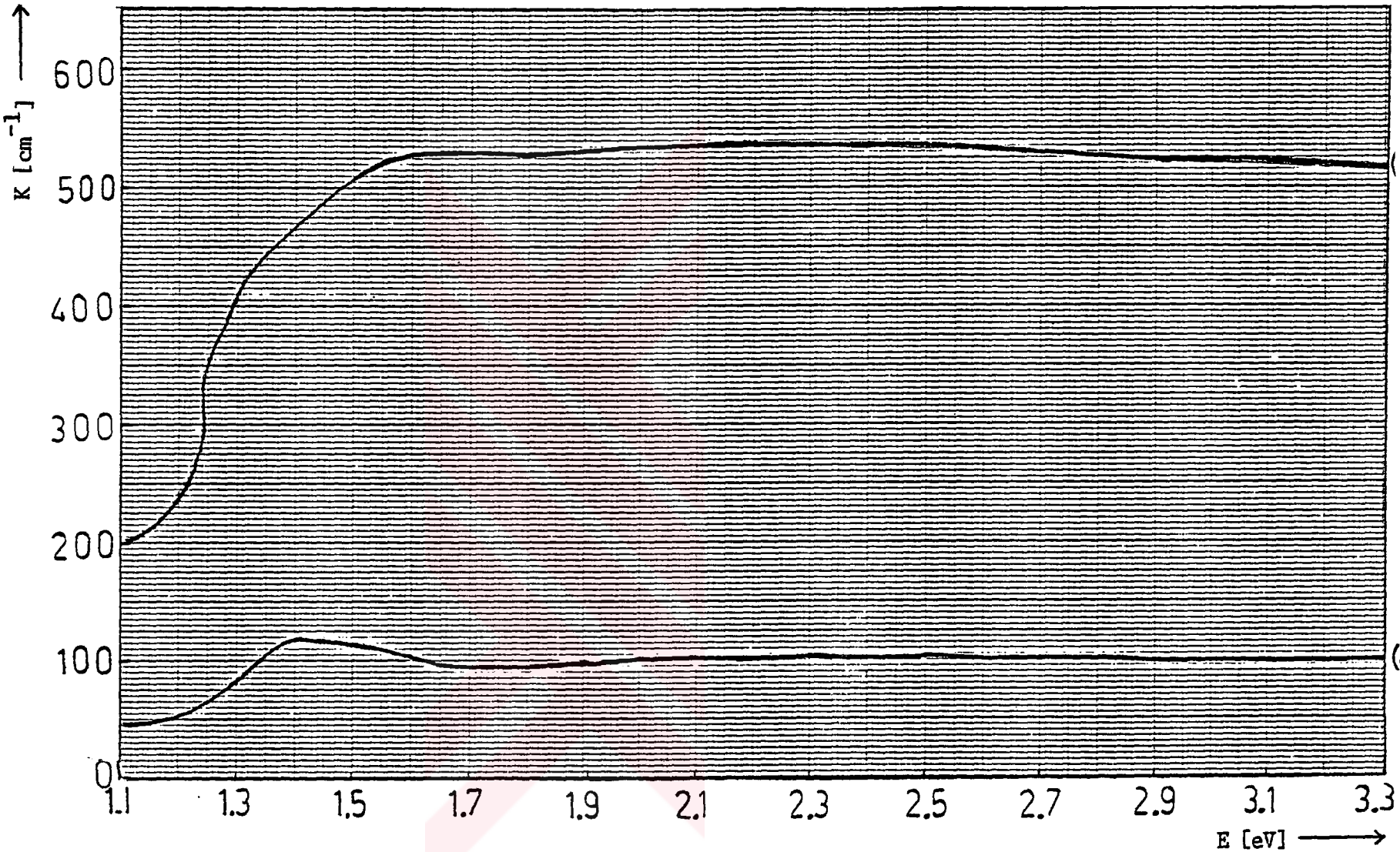

Fig.7b K versus E of SnSe for $\varepsilon \| \vec{a}$ and $\varepsilon \| \vec{b}$ polarisations.

indirect bandgap energy of SnSe. These graphs have been drawn for the polarisations of $\vec{a}$ and $\vec{b}$ in the cleavage plane. The dependence of $(KE)^{1/2} = f(E)$ was approximately linear in the energy range of about 1.12 to 1.46 eV and 1.12 to 1.31 eV for the polarisations of $\mathcal{E} \| \vec{a}$ and $\mathcal{E} \| \vec{b}$ respectively. The dependence of $(KE)^{1/3} = f(E)$ was also found to be linear in the energy range of about 1.12 to 1.49 eV and 1.12 to 1.40 eV for the polarisations of $\mathcal{E} \| \vec{a}$ and $\mathcal{E} \| \vec{b}$ respectively. Two different graphs have been used, in order to obtain more accurate results for the bandgap energy of SnSe. From the analysis of these two graphs, the bandgap energy of SnSe was found E'_a = 0.92 eV and E''_a = 0.57 eV for $\mathcal{E} \| \vec{a}$ polarisation. Similarly, the bandgap energy of SnSe was found E'_b=0.98 eV and E''_b =0.62 eV for $\mathcal{E} \| \vec{b}$ polarisation. The bandgap energies of E'_a and E'_b were obtained from figure 8 whereas E''_a and E''_b were obtained from figure 9. In order to obtain more reliable and accurate values of E'_a and E''_a for $\mathcal{E} \| \vec{a}$ polarisation and E'_b and E''_b for $\mathcal{E} \| \vec{b}$ polarisation have been averaged. Finally, the values of bandgap energies have been found E_a = 0.74 eV and E_b =0.8 eV for polarisations of $\mathcal{E} \| \vec{a}$ and $\mathcal{E} \| \vec{b}$ respectively.

The situation was complicated at higher energies. Because the precision of the determination of the character of the transition depends on the correct estimation of absorption coefficient, K, whereas K characterises lower energy transitions.

Figure 10 was also obtained by drawing $(KE)^{1/2}$ versus E in an energy range of about 1.1- 1.4 eV in order to obtain the first and second indirect transitions, E_{i1} and E_{i2} respectively. This dependence of

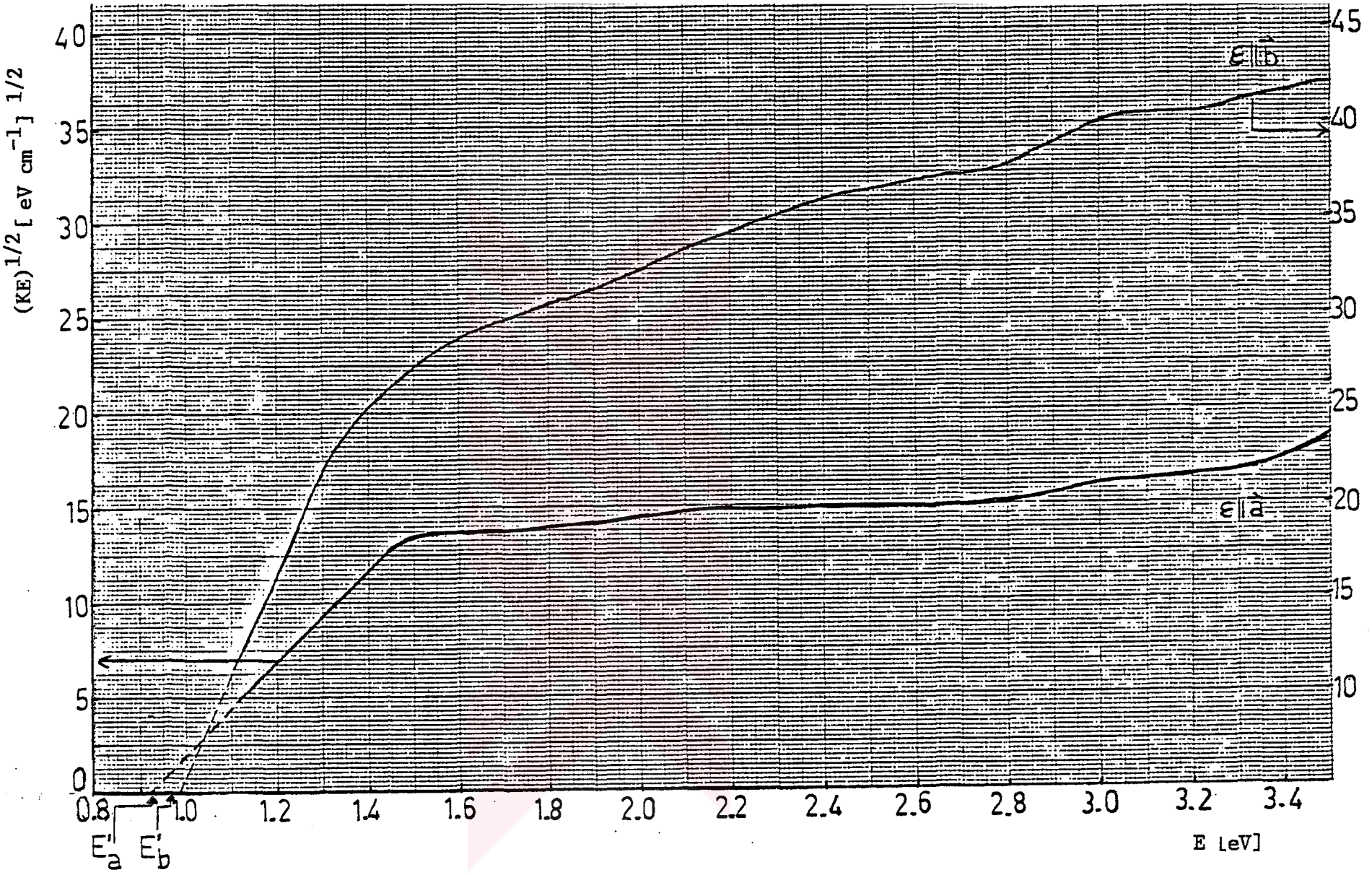

Fig.8 $(KE)^{1/2}$ versus E of SnSe for $\varepsilon \| \vec{a}$ and $\varepsilon \| \vec{b}$ polarisations.

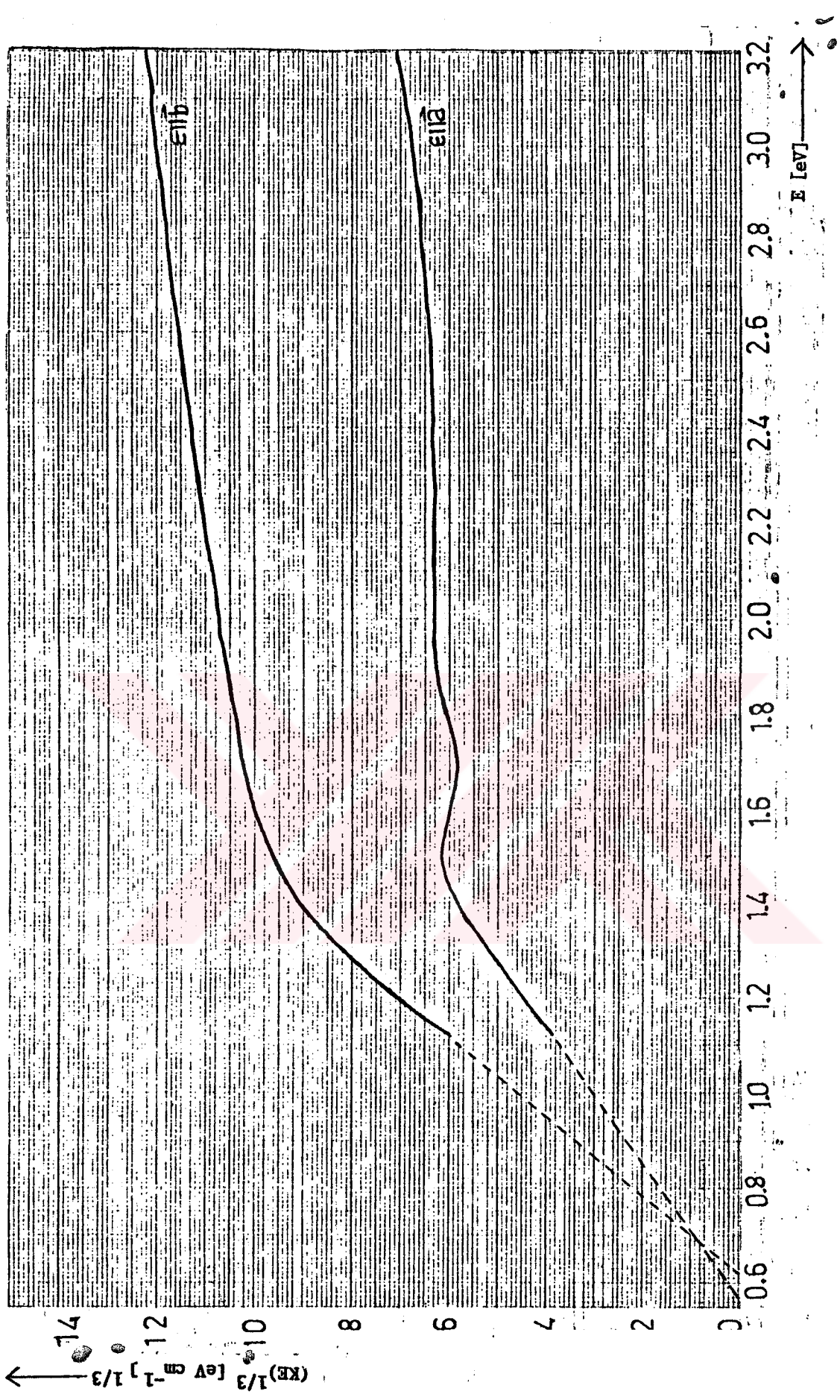

Fig.9 $(KE)^{1/3}$ versus E of SnSe for $\varepsilon \| \vec{a}$ and $\varepsilon \| \vec{b}$ polarisations.

$(KE)^{1/2} = f(E)$ gave results in terms of E_{i1} =1.14 + 0.01 eV and E_{i2} = 1.26 + 0.012 eV for $\mathcal{E} \| \vec{a}$ polarisation and E_{i1} =1.12 + 0.01 eV and E_{i2} =1.22 +0.01 eV for $\mathcal{E} \| \vec{b}$ polarisation.

A pronounced break on the K= f(E) curve (fig. 11.a) was observed for polarisation $\mathcal{E} \| \vec{a}$. It was identified that this break was the first direct transition for $\mathcal{E} \| \vec{a}$ with an energy of E_{1d} = 1.30 + 0.01 eV. As it can be seen from figure 11.b that the absorption coefficient starts to increase very rapidly at E_{1d}=1.29 +0.01 eV at room temperature. This energy, E_{1d} , was identified as the first direct interband transition for $\mathcal{E} \| \vec{b}$ polarisation.

4.3 Tin Sulphide (SnS)

In figure 12 the variation of absorption coefficient corresponding to the specific wavelength was presented for the two directions of polarisation at room temperature. Thus, the difference of the absorption coefficient for the two directions of polarisation was greater in the vicinity of the absorption edge.

Plotting the square root of the quantity $(Kh\nu)$ vs $h\nu$, a straight line was expected to resolve for each independent processes. Such a plot for tin sulphide was presented in figure 13.

In order to examine the complex absorption processes, figure 14 was obtained by drawing $\partial (Kh\nu)^{1/2} / \partial (h\nu)$ which was suggested by Koshkin et al.[23]. This method has been employed using graphical differentiation of the data presented in figure 13 for the two

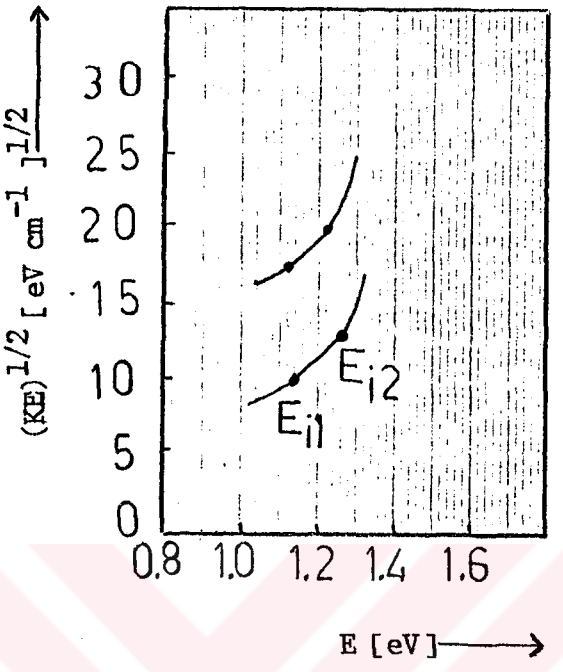

Fig.10 $(KE)^{1/2}$ versus E of SnSe in polarised light at room temperature.

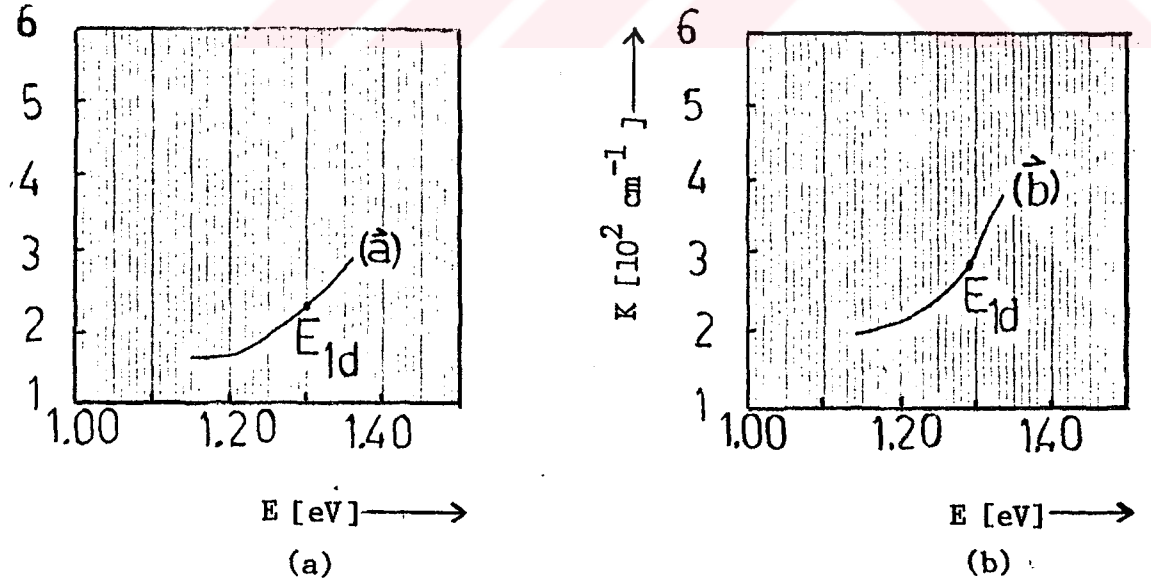

Fig.11 K versus E of SnSe in polarised light for a) $\mathcal{E}\|\vec{a}$ and b) $\mathcal{E}\|\vec{b}$.

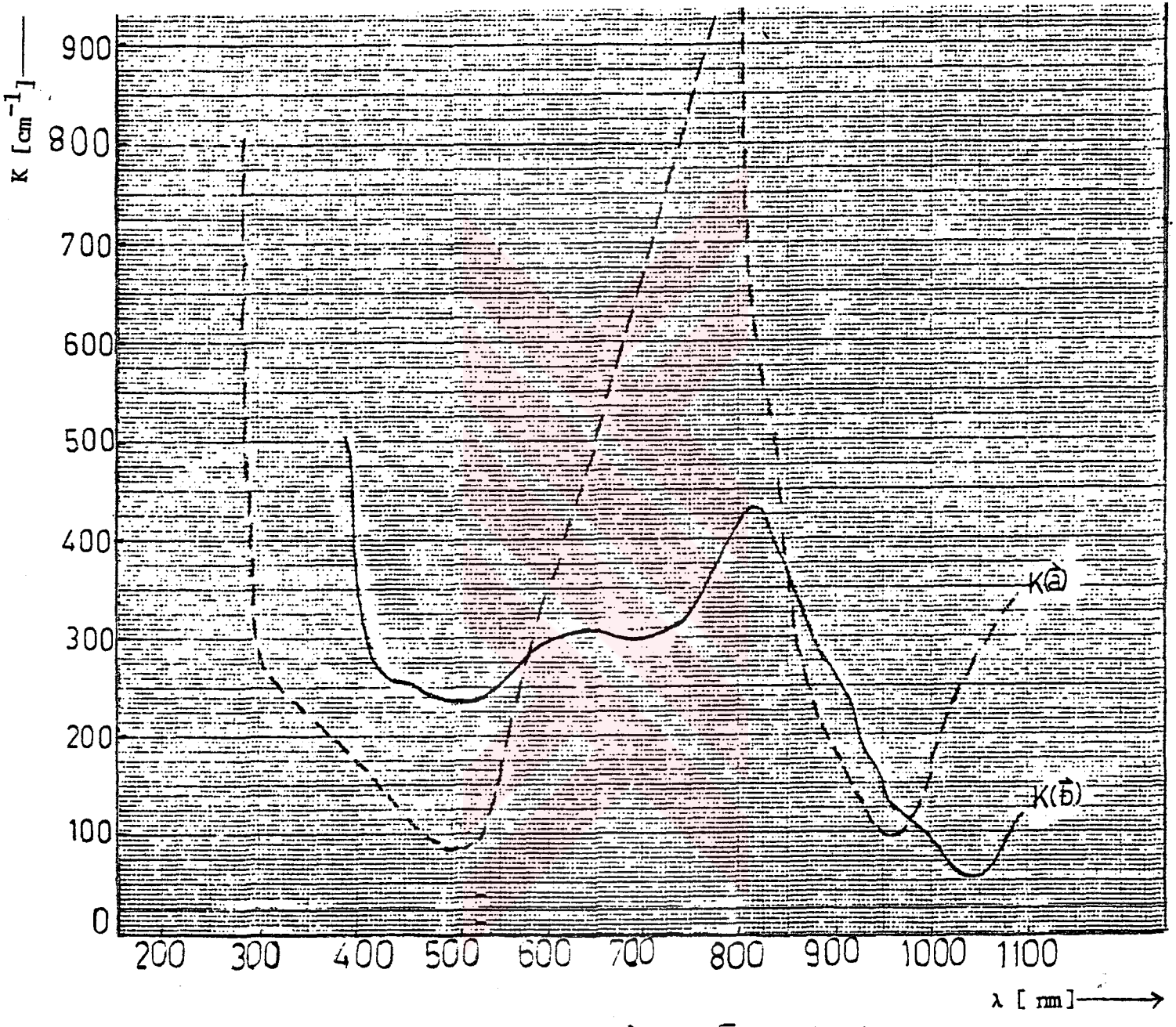

Fig.12 K versus λ of SnS for $\varepsilon \parallel \vec{a}$ and $\varepsilon \parallel \vec{b}$ polarisations.

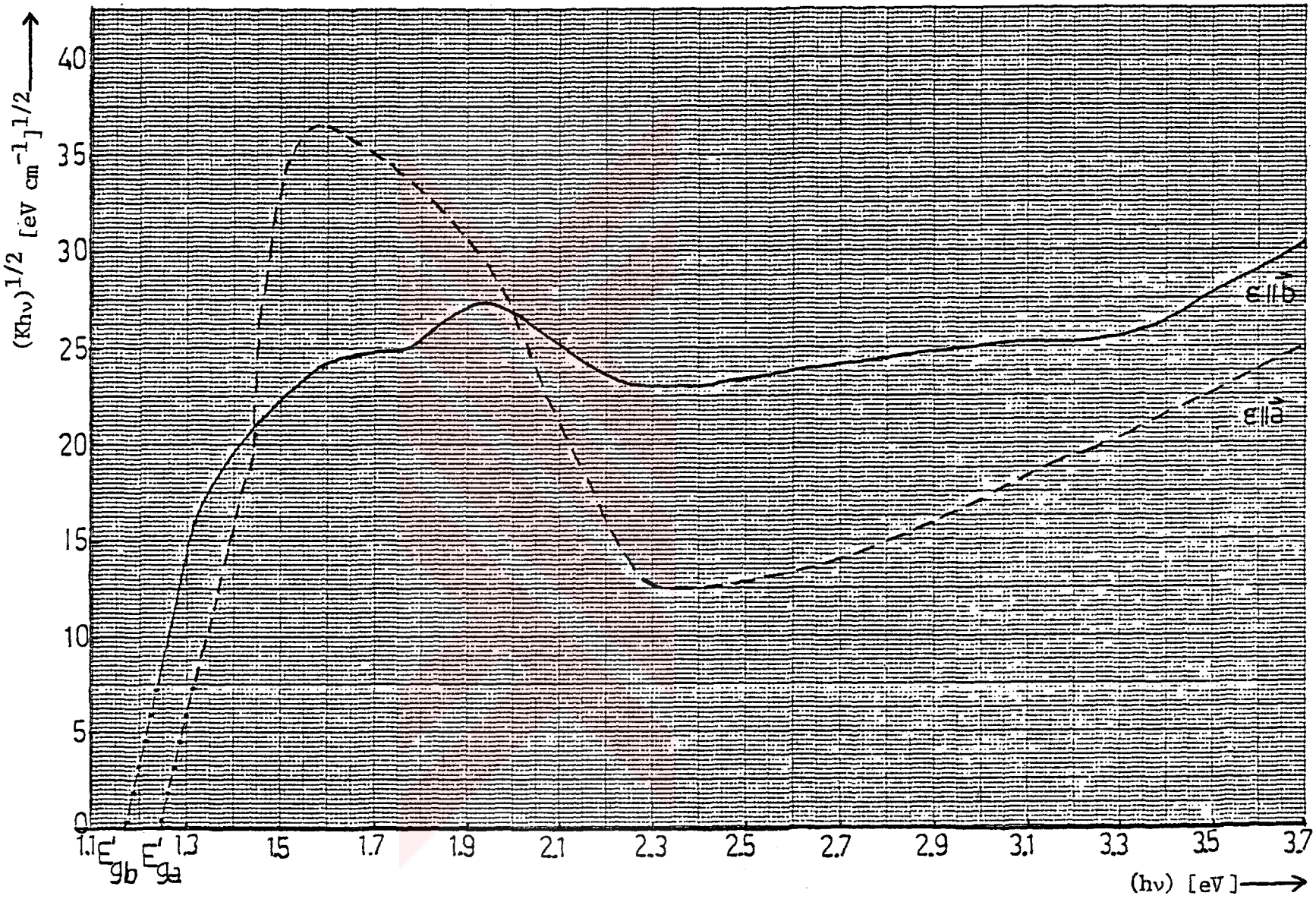

Fig.13 $(Kh\nu)^{1/2}$ versus hν of SnS for $\varepsilon \| \vec{a}$ and $\varepsilon \| \vec{b}$ polarisations.

directions of polarisations of $\mathcal{E}||\vec{a}$ and $\mathcal{E}||\vec{b}$.

As it was evident from these figures, the derivative $\partial(Kh\nu)^{1/2} / \partial(h\nu)$ was a step function of energy, with four steps

$$E_o < h\nu < E_1$$
$$E_1 < h\nu < E_2$$
$$E_2 < h\nu < E_3$$
$$E_3 < h\nu$$

where these energy values E_o ,E_1 ,E_2 , and E_3 indicate the points of discontinuity in the plot of figure 14. It was known from the theory that the dependence of absorption coefficient on energy can be described by equation 3.11, which as follows

$$(kh\nu)^{1/2} = b_o + \sum_{i=1}^{n} b_i(h\nu - E_g' \pm E_i)$$

where b_i indicates the difference in the height of the steps in the plots of figure 14. E_g' was the energy value of the indirect band gap and E_i was the energy of the phonon involved in the process. Values of constants b_i , and the energy values of the points of discontinuity, E_i , for the two directions of polarisations were given in Table 7 at room temperature. Since four steps was observed, there was two different phonons participating in the absorption process. Indirect energy gap values were calculated using equations 3.12, and phonon energies were calculated using equations 3.13. The energy of the indirect band gap can be estimated also from the intercept of the straight line, representing the data in figure 13 with the energy axis.

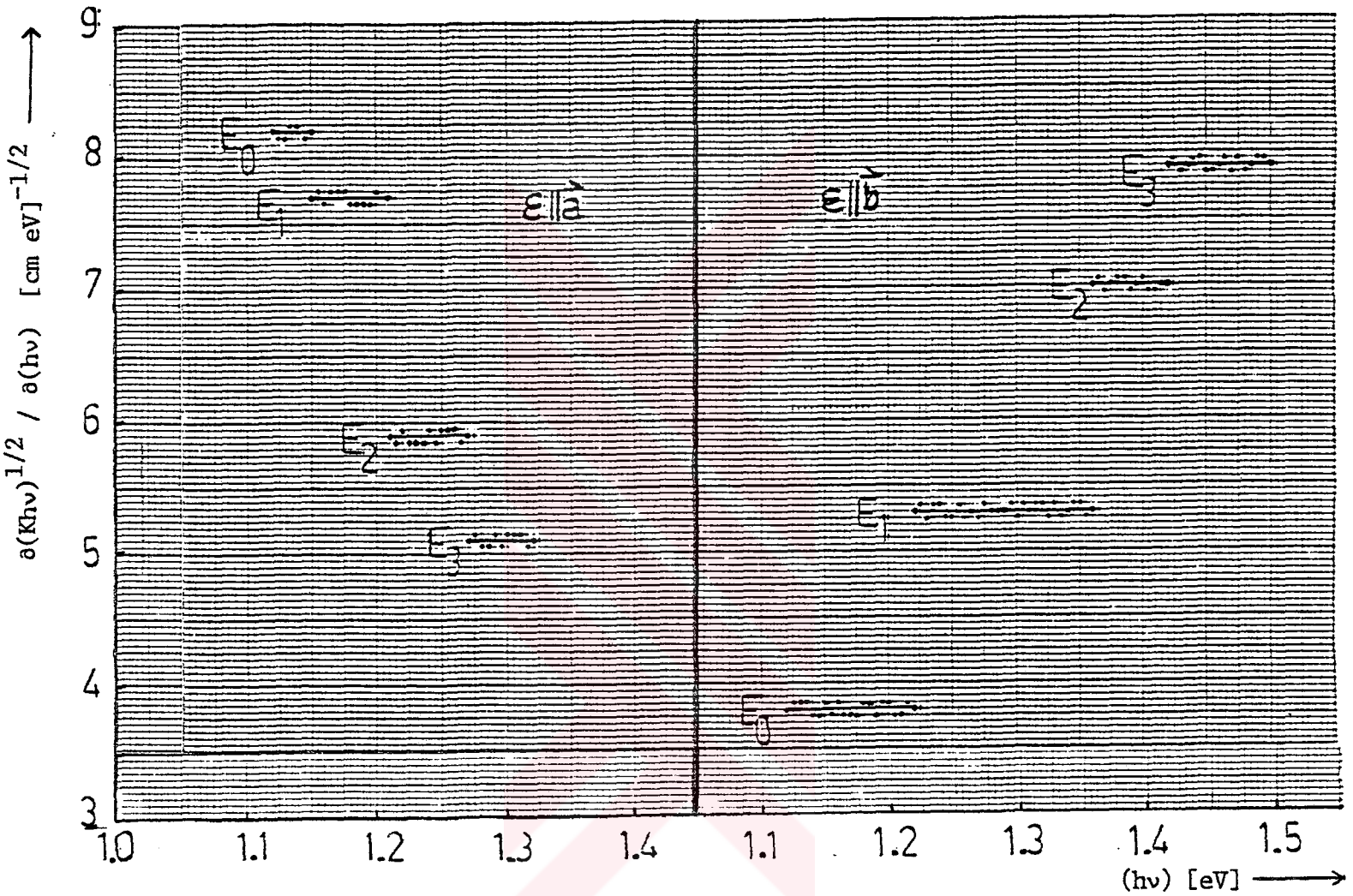

Fig.14 $\alpha(K h\nu)^{1/2} / \alpha(h\nu)$ versus $h\nu$ of SnS for $\varepsilon \| \vec{a}$ and $\varepsilon \| \vec{b}$ polarisations.

Table 7. Steepness coefficients and energy values of the points of discontinuity for the absorption edge of SnS for two directions of light polarisations at 300 K.

	$\varepsilon \parallel \vec{a}$	$\varepsilon \parallel \vec{b}$
E_o (eV)	1.12	1.12
E_1 (eV)	1.15	1.22
E_2 (eV)	1.21	1.36
E_3 (eV)	1.27	1.42
b_o (cm eV)$^{-1/2}$	8.2	3.8
b_1 (cm eV)$^{-1/2}$	0.5	1.5
b_2 (cm eV)$^{-1/2}$	1.8	1.7
b_3 (cm eV)$^{-1/2}$	0.8	0.9
b_4 (cm eV)$^{-1/2}$	5.1	7.8

Table 8. Indirect bandgap energy and energy of phonons for SnS.

	$\varepsilon \parallel \vec{a}$	$\varepsilon \parallel \vec{b}$
E'_g (eV)	1.22	1.15
E'_{g03} (eV)	1.195	1.27
E'_{g12} (eV)	1.18	1.29
β_1 (eV)	0.03	0.05
β_2 (eV)	0.075	0.15

CHAPTER FIVE

DISCUSSION AND CONCLUSION

5.1 Discussion

The following effects have been found from the investigation of the transmissivity of SnS and SnSe samples at room temperature:

a) In the plot of absorption coefficient K versus Wavelength for $\mathcal{E} \| \vec{a}$ polarisation, only one absorption band at around 750 nm (1.65 eV) was observed, compared to the two absorption bands at around 815 nm (1.52 eV) and 625 nm (1.986 eV) for the measurement of $\mathcal{E} \| \vec{b}$ polarisation in the same graph (see fig.12). Since the impurity content of the SnS crystal was not known it would be difficult to specify the origin of the strong absorption band observed for $\mathcal{E} \| \vec{a}$ polarisation. This peak could well be due to the transition of the electrons either from the valence band to an impurity centre near the conduction band or the transition of electrons from an impurity centre to the conduction band.

b) The relatively weaker absorption band observed at around 815 nm for the $\mathcal{E} \| \vec{b}$ polarisation was found to be in good agreement with the theory that the absorption bands for $\mathcal{E} \| \vec{b}$ polarisation should be smaller than that of the absorption peaks for $\mathcal{E} \| \vec{a}$ polarisation.

c) The second absorption band which was observed for $\mathcal{E} \| \vec{b}$ polarisation seemed even weaker than the first peak and it was not observed in the curve which was drawn for the $\mathcal{E} \| \vec{a}$ polarisation.

d) There seems an indication of an increase in the absorption coefficient graph in the near infrared region which is beyond the measurement range of our system and it would be very difficult to interpret this behaviour.

e) A similar graph which was drawn for SnSe (see fig.-7.b) has shown a very different characteristic compared to the one drawn for SnS. In this figure the absorption coefficients for $\mathcal{E} \parallel \vec{a}$ and $\mathcal{E} \parallel \vec{b}$ polarisations have shown a sharp increase following the wavelength values corresponding to the absorption edge and for the shorter wavelengths the absorption coefficients remained constant throughout the whole range of measurements.

The bandgap of SnS which was found 1.24 eV and 1.17 eV for $\mathcal{E} \parallel \vec{a}$ and $\mathcal{E} \parallel \vec{b}$ polarisations respectively in this study seemed in reasonably good agreement with the values of 1.142 and 1.095 eV obtained by Lambros et al. [4]. They have also used transmissivity measurements in the determination of the bandgap of SnS and have used $\mathcal{E} \parallel \vec{a}$ and $\mathcal{E} \parallel \vec{b}$ polarisations in their experiments. Bandgap values of 1.24 and 1.17 eV found in the present study, were also in good agreement with the values of 1.2 eV obtained by Anderson and Morton [2], 1.25 eV obtained by Gobrecht and Bartchat [21] and 1.07 eV obtained by Albers et al. [16]. It should be noted that Anderson and Morton have found the bandgap value by electrical measurements and Gobrecht and Bartchat have found by photoconductivity measurements. Both studies concerning with the bandgap of SnS have not distinguished the result for $\mathcal{E} \parallel \vec{a}$ and $\mathcal{E} \parallel \vec{b}$ polarisations but instead they have given only one single value for the bandgap of SnS. Albers et al. have

studied the optical behaviour of SnS in the vicinity of the absorption edge by using unpolarised light and a similar graph (plot of square root of absorption coefficient versus photon energy) provided in this study. As a result, they have also produced one single value for the bandgap of SnS irrespective of $\mathcal{E} \| \vec{a}$ and $\mathcal{E} \| \vec{b}$ polarisations.

Similar to the measurements of SnS, the bandgap of SnSe has been found 0.74 and 0.8 eV for $\mathcal{E} \| \vec{a}$ and $\mathcal{E} \| \vec{b}$ polarisations respectively in this present study. The bandgap values of SnSe were obtained from the $(KE)^{1/2}$ versus E and $(KE)^{1/3}$ versus E graphs by averaging the bandgap values for each polarisations (see figs.8 and 9). The bandgap values of 0.907 and 1.01 eV reported by Lukes et al. [16] indicated that the difference in the values of bandgap energies for $\mathcal{E} \| \vec{a}$ and $\mathcal{E} \| \vec{b}$ polarisations much higher than that of found in this study. Nevertheless, when the individual values for each polarisations were taken into account, the differences in the values of the bandgap energies were in the acceptable limits of the experimental measurements.

The $K_a < K_b$ relation was found to be valid for the whole range of photon energies in the transmissivity measurements of SnSe which is in agreement with all the other reports [4,6,9.22]. In the measurements of SnS $K_a > K_b$ relation was found to be valid for the whole range of wavelengths and this is in quite good agreement with other reports mentioned in the previous sentence. The only exception to this was reported by Valiukonis et al. [23] in which the $K_a < K_b$ relation was suggested.

5.2 Conclusion

The indirect bandgap of SnS was found to be 1.24 eV and 1.17 eV for $E \| \vec{a}$ and $E \| \vec{b}$ polarisations respectively. Similarly the indirect bandgap of SnSe was found to be 0.74 and 0.81 eV for $E \| \vec{a}$ and $E \| \vec{b}$ polarisations respectively.These values were also confirmed by other authors who have found the bandgaps by using similar and/or different methods.

All the results found in this study have indicated that the absorption edges for SnS and SnSe were characterised by indirect transitions. Indirect transitions could be either allowed and/or forbidden. No distinction could be possible under the circumstances.

The $K_a < K_b$ relation was found to be valid for whole range of energies of incident light for SnSe but $K_a > K_b$ for SnS. This result seemed to be in a very good agreement with almost all of the reports made by the workers in this field.

It has been found that there were at least two indirect transitions before the onset of absorption due to the direct transition for SnSe.

The experimental results obtained in this study were confined only for $E \| \vec{a}$ and $E \| \vec{b}$ polarisations where $\vec{a}$ and $\vec{b}$ were lying in the cleavage plane. Because of the reasons mentioned in chapter 1, no data were presented for $\vec{c}$ polarisation in this study.

It was also found that, the phonon assisted indirect transitions in SnS require the participation of two phonons with energies of 0.03 and 0.075 eV for $E \| \vec{a}$ polarisation and 0.05 and 0.15 eV for $E \| \vec{b}$ polarisation.

The optical behaviour of SnS and SnSe was found to be strongly anisotropic during the course of this study.

REFERENCES

1. W. Hoffmann, Z. Kristallogr. 92 (1935) 161.
2. F. Lukes, P. Dub, Univerzita J.E. Purkyne V. Brne. (1988)
3. I. Gregore, B. Velicky, and Zavetova, J. Phys. Chem. Solids 37 (1976) 785.
4. A.P. Lambros, D. Geraleas, and N.A. Economov, J. Phys. Chem. Solids, 35 (1974) 537.
5. N.Ch. Abrikosov and L.E. Shelimova, Semiconducting Materials on the basis of IV-VI compounds, (1975).
6. R. Eymard and A. Otto, Phys. Rew. B 16 (1977) 1616.
7. V.V. Sobolev and V.I. Donetskich, Neorganitcheskie Materialy (inorganic materials) VIII, (1972) 688.
8. D.I. Bletskan, A.M. Eustigneev, I.F. Kopinec, I.M. Migolinec, V.A. Tyagai, Neorganitcheskie Materially, 10 (1974) 735.
9. V.A. Tyagai, V.N. Bondarenko, A.N. Krasiko, D.I. Bletskan, and V.I. Sheka, Tela Fiz. Tverd, Soviet Physics-Solid State, 18 (1976) 1433.
10. T. Arai, M. Onomichi, Y. Mochida, and K. Kudo, Proc. Internat. Conf. Physics and Chemistry of Semiconductors, 4 (1971) 51.
11. A.K. Gark, A.K. Jain, and O.P. Agnihotri, Indian J. Pure Appl. Physics. 21 (1983) 273.
12. J.G. Yu, A.S. Yue, and O.M. Stafsudd, J. Crystal Growth, 54 (1981) 248.
13. G. Valiukonis, F.M. Gashimzade, D.A. Guseinova, G. Krivaite, M.M. Mamedov, A. Sileika, Phys. Stat.Sol. (B), 122 (1984) 623.
14. F. Lukes, E. Schmidt, J. Humlicek, P. Dub and F. Kosek, Phys. Stat. Sol. (B), 137 (1986) 569.

15. S.V. Vlachos, A.P. Lambros, N.A. Economou, Solid State Communication, 19 (1976) 759.
16. W. Albers, C. Haas, and E. Van der Maesen, J. Phys. Chem. Solids, 15 (1960) 306.
17. V.M. Koshkin, V.R. Karas, L.P. Cal'chinetskii, Sov. Phys.-Semicond. , 3 (1970) 1186.
18. G. Ciucci, A. Guarnieri, G.L. Masserini, L. Quart pelle, Solid State Commun. 29 (1979) 75.
19. G. Valiukonis, F.M. Gashimzade, D.A. Guseinova, G.Z. Krivaite, M.M. Mamedov, and A. Sileika, Liet. Fiz. Rink., 25 (1985) 39.
20. H.R. Chandarsekhar, R.G. Humphreys, U. Zwick,and M. Cardona, Phys. Rew. B, 15 (1977) 2177.
21. H. Gobrecht and A. Bartschat, Z. Phys., 149 (1957) 511.
22. F. Lukes, J. Humlicek, and E. Schmidt, Solid State Commun., 45 (1983) 445.
23. G. Valiukonis, D.A. Gusinova, G. Krivaite, and A. Sileika, Phys. Stat. Sol. (B), 135 (1986) 299.
24. F.M. Gashimzade, Tela Fiz. Tverd, (Soviet Phys.-Solid State), 2 (1960) 2070.